THREE-DIMENSIONAL MODELLING OF HIGH-POWER LASER DIODES BASED ON THE FINITE INTEGRATION BEAM PROPAGATION METHOD

Monika Niederhoff [1], Wolfgang Heinrich [1], and Peter Russer [2]

[1] Ferdinand-Braun-Institut für Höchstfrequenztechnik, Berlin, Germany, Rudower Chaussee 5, D-12489 Berlin, Germany, phone +49 30 63922628, fax +49 30 63922602

[2] Lehrstuhl für Hochfrequenztechnik, Technische Universität München, Arcisstr. 21, D-80333 München, Germany, phone +49 89 21058390, fax +49 89 21053365

ABSTRACT

A self-consistent three-dimensional method for modelling high-power laser diodes is presented, that is based on the finite integration beam propagation method (FIBPM). It allows the modelling of longitudinally inhomogeneous lasers, and takes into account the influence of the distributions of the injection current, the carrier density and the temperature profile. The method has been applied to various high-power laser diode structures. Simulation results have been verified by experimental data.

INTRODUCTION

High-power semiconductor lasers meet with growing interest in numerous applications, e. g. as pump sources for solid-state lasers and fiber optical amplifiers, and in optical measurement and communication systems [1]. In these lasers very long cavities are employed in order to obtain high output power. In this way sufficient amplification of the propagating optical wave is guaranteed. Consequently a longitudinally strongly inhomogeneous optical field distribution will evolve within the cavity even in cases where the laser structure is a priori longitudinally homogeneous. Therefore, three-dimensional modelling of the propagating electromagnetic field and the nonlinear laser effects is required for the design and optimization of high-power semiconductor lasers.

For this reason, we have developed a *three-dimensional* laser model. This model is based on the finite-integration beam propagation method (FIBPM) [2, 3]. Compared to [2, 3], the following new features, that result in a nonlinear behavior, are introduced: interaction of the optical field with the carrier density, influence of current spreading, and dependence on temperature profile. Contrary to previous two-dimensional methods (e.g. [4, 5]), our novel model allows the developement and optimization of complex laser diodes that contain transversal as well as longitudinal structuring.

The laser model is described in the following section. In the subsequent section results are presented that were obtained by applying the model to a RISAS laser.

TH 2D

THE FIBPM LASER MODEL

Figure 1 shows the nonlinear interaction of the physical quantities that are taken into consideration in the presented laser modell. From the contact the current flows to the active zone. The current distribution in the p-doped region above the active zone is determined by the electrical conductivity σ and the quasi fermi levels E_n^{F} and E_p^{F} of electrons and holes in the active zone. The injection current density J_{i} in the active zone creates the carrier profiles n_{c} and p, who depend additionally on recombination rates, diffusion and drift. The optical gain is determined by the carrier profile in the active zone. Furthermore, the carrier density influences the real part of the refractive index in the active zone. The guidance of the optical field depends on the distribution of the complex refractive index, whose imaginary part is determined by the optical gain as well as by absorption losses. The optical power density interacts with the carrier density in the

0-7803-3246-6/96/$5.00 © IEEE

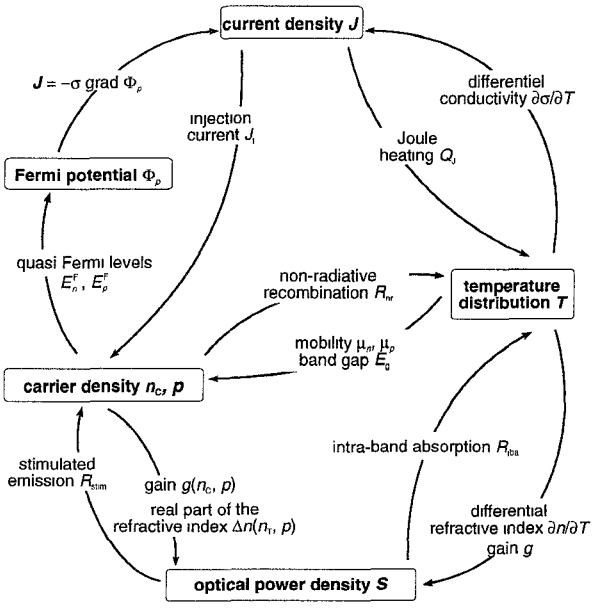

Fig. 1: Nonlinear interaction in semiconductor lasers.

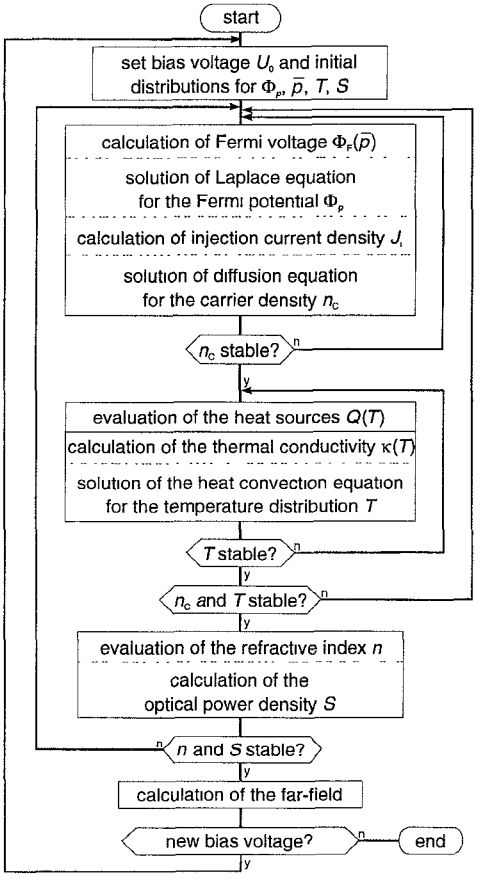

Fig. 2: Algorithm for the self-consistent solution of the laser equations

active zone because of the stimulated emission. Additionally, this system of nonlinear interaction is influenced by the temperature distribution, as indicated in fig. 1.

The model for the numerical simulation of these nonlinear interactions is based on the FIBPM. The FIBPM is a full-vector beam propagation method, that allows the calculation of the propagating electromagnetic field in longitudinally inhomogeneous optical waveguides [2, 3]. The transversal field discretization is based on finite integration [8]. This method is especially suited for structures containing very thin layers such as quantum wells. The FIBPM is based on the paraxial approximation. This means, that the coupling of forward and backward travelling waves is neglected. For the FIBPM, a code for running the simulation on a massively parallel computer was developed that allows a very efficient calculation of the field propagation.

The calculation of the distributions of current and carriers is based on the assumption that the resistivity of the n-doped layers underneath the active zone is neglectable in comparison to the resistivity of the p-doped layers above the active zone ($\sigma_n \rightarrow \infty$). The current density J is calculated by solving the Laplace equation for the Fermi potential Φ_p in the p-doped region. The carrier density n_c is evaluated by solving an effective diffusion equation in the active zone according to the model introduced by Joyce [6]. The temperature profile is calculated by solving the heat convection equation. The numerical solution of these three equations is based on discretization by finite differences.

For simulating the behaviour of semiconductor lasers the algorithm in fig. 2 is applied. In longitudinal direction the cavity is subdivided into several sections that are assumed to be approximately homogeneous. For each section, the Laplace equation, the diffusion equation, and the heat convection equation are solved in the transversal plane in the middle of that section. From the solution of these equations a modified transversal profile of the complex refractive index is obtained for each cavity section, thus yielding a longitudinally inhomogeneous waveguide structure. The electromagnetic field distribution is determined by evaluating the propagation of the wave along the cavity — backward and forward. After each cycle the

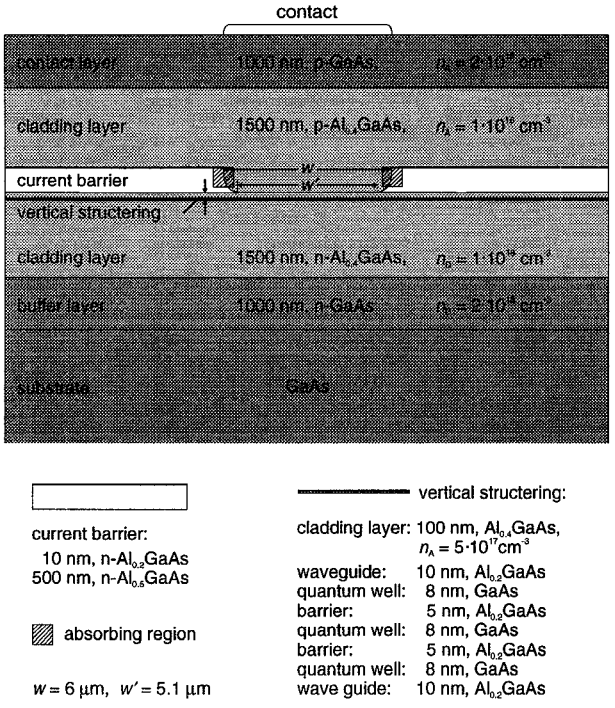

Fig. 3: Structure of the RISAS-Lasers on which the simulations in this paper are based, (length of cavity $L = 800\,\mu$m, mirror reflectivities $R_1 = 0.03$, $R_2 = 0.96$).

profile of the complex refractive index is updated by solving the Laplace equation, the diffusion equation, and the heat convection equation until a stable distribution for all the relevant quantities is obtained.

RESULTS: RISAS LASER

In this section results are presented that were obtained by applying the described laser model to a RISAS (real index guided self alignmant structure) laser. For this laser experimental results were given in [7]. Therefore, our laser model could be verified by comparing the results of the simulation with the experimental data from [7]. Figure 3 shows the structure of the cross section of this laser.

In fig. 4 the transversal distribution of the optical near field of the fundamental mode is depicted. When the current/power characteristic of this structure is calculated self-consistently, a higher order mode appears at $P_{\text{opt}} \approx 100\,\text{mW}$ because of spatial hole burnung effects. In the experiments presented in [7] this higher order mode only appears at $P_{\text{opt}} > 600\,\text{mW}$. This

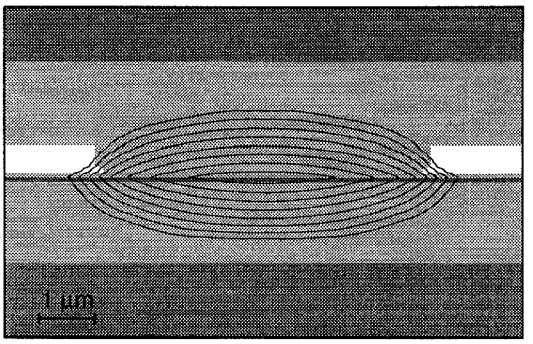

Fig. 4: Transversal near field distribution of the optical power density of the fundamental mode in the RISAS laser in fig. 3 (contour lines at 0.005, 0.01, 0.02, ..., 0.64).

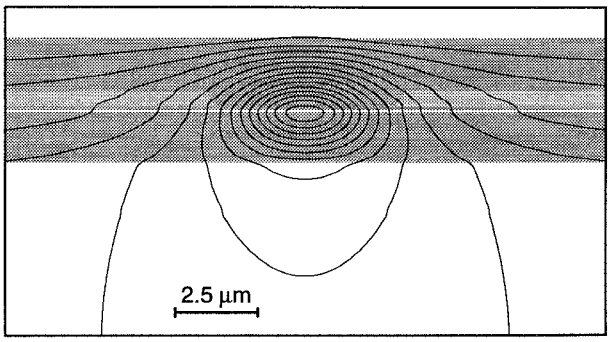

Fig. 5: Temperature distribution in the transversal plane $z = 80\,\mu$m of the RISAS laser in fig. 3 ($P_{\text{opt}} = 612\,\text{mW}$, contour lines at 301, 302, ..., 314 K).

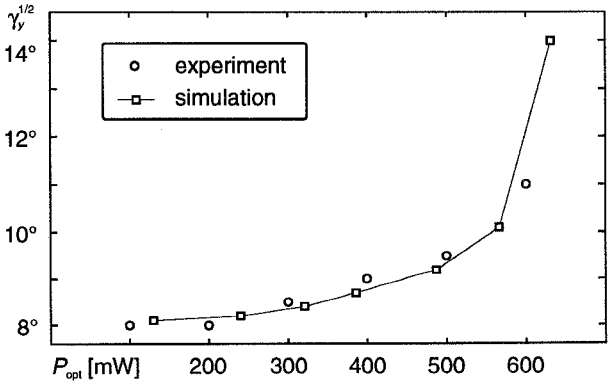

Fig. 6: Comparison of measured [7] and calculated values for the lateral far-field divergence for the RISAS laser in fig. 3.

deviation could be explained by losses in the region of the etching edges that affect the higher order mode more strongly than the fundamental mode. In order to suppress the higher order mode in the simulations in a way that corresponds to the experimental results, absorbing zones ($\alpha = 800\,\mathrm{cm}^{-1}$) were introduced in the region of the etching edges as indicated in fig. 3. In this way, the output power 612 mW in single mode operation was obtained in the simulations. The calculated threshold current is $I_{\mathrm{th}} = 40\,\mathrm{mA}$, the gradient of the current/power characteristic is $\Delta P/\Delta I = 1.4\,\mathrm{mW/mA}$. The deviation from the experimental results ($I_{\mathrm{th}} = 36\,\mathrm{mA}$, $\Delta P/\Delta I = 1.3\,\mathrm{mW/mA}$) is about 10%. Figure 5 shows the temperature distribution in the cross section $z = 80\,\mu\mathrm{m}$ of the RISAS laser at the output power $P_{\mathrm{opt}} = 612\,\mathrm{mW}$.

With growing output power the near-field width in lateral direction becomes smaller because of self-focussing. This effect is due to heating and carrier depletion, both of which cause a rise in the refractive index in the central region of the structure. When the near-field width decreases, the far-field divergence increases. Figure. 6 shows that the experimental results for the power dependence of the far-field divergence are in good agreement with the simulations.

CONCLUSIONS

A self-consistent model for the three-dimensional simulation of semi-conductor lasers has been presented. The nonlinear effects caused by the interaction of the optical field with the current distribution, the carrier density, and the temperature profile are included in this modell. The model has been applied to various structures that are typical for the design of high power laser diodes. As an example, in this paper result for a RISAS laser are presented. A comparison with experimental results proves the validity and the accuracy of the model. This is true especially for those effects concerning the waveguiding properties of the laser cavity that depend on the nonlinear interaction of the optical field with the carrier density and the temperature profile.

ACKNOWLEDGEMENTS

We wish to thank the Deutsche Forschungsgemeinschaft (DFG) for supporting this work under grant Ru 314/26.

REFERENCES

[1] Y. Suematsu, A. R. Adams, "Handbook of semiconductor lasers and photonic integrated circuits". *Chapman & Hall*, London (1994).

[2] M. Niederhoff, W. Heinrich, P. Russer, "Three-dimensional full-vector analysis of optical waveguides by finite-integration beam-propagation method". *Int. Journal of Numerical Modelling, in print.*

[3] M. Niederhoff, W. Heinrich, P. Russer, "The Finite-Integration Beam-Propagation Method". *1995 IEEE MTT-S International Microwave Symposium Digest* **2**, Orlando, May 16–20 1995, pp. 483–486.

[4] G.-L. Tan, N. Bewtra, K. Lee, J. M. Xu, "A two-dimensional nonisothermal finite element simulation of laser diodes". *IEEE J. Quantum Electron.* **29** (3), (1993), S. 822–835.

[5] M. Grupen, U. Ravaioli, A. Galick, K. Hess, T. Kerkhoven, "Coupling the electronic and optical problems in semiconductor quantum well laser simulations". *Physics and Simulation of optic devices — SPIE* **2146**, (1994), S. 133–147.

[6] W. B. Joyce, "Carrier transport in double-heterostructure active layers". *J. Appl. Phys.* **53** (11), (1982), S. 7235–7239.

[7] O. Imafuji, T. Takayama, H. Sugiura, M. Yuri, H. Naito, M. Kume, K. Itoh, "600 mW CW single-mode GaAlAs Triple-Quantum-Well Laser with a New Index Guided Structure". *IEEE J. Quantum Electron.* **29** (6), (1993), S. 1889.

[8] T. Weiland, "Zur numerischen Lösung des Eigenwellenproblems längshomogener Wellenleiter beliebiger Randkontur und transversal inhomogener Füllung ". *Dissertation TH Darmstadt*, (1977).